# Entropic barriers determine adiabatic electron transfer equilibrium

**Eric J. Piechota[‡,1], Renato N. Sampaio[‡,†,1], Ludovic Troian-Gautier[1], Andrew B. Maurer[1], Curtis P. Berlinguette[2], and Gerald J. Meyer[*,1]**

[1] *Department of Chemistry, University of North Carolina at Chapel Hill, Murray Hall 2202B, Chapel Hill, North Carolina 27599, United States*

[2] *Departments of Chemistry and Chemical & Biological Engineering, and the Stewart Blusson Quantum Matter Institute, The University of British Columbia, 2036 Main Hall, Vancouver, British Columbia V6T 1Z1, Canada*

**ABSTRACT:** A thermodynamic analysis of the forward and reverse rate constants for adiabatic and nonadiabatic electron transfer equilibria over an 80 K temperature range is reported. The kinetic data were acquired by a spectroscopic approach that utilized excited state injection into $TiO_2$ by sensitizers with two redox active groups linked through aromatic bridges that allow for intramolecular adiabatic (bridge = **p**henyl) or nonadiabatic (bridge = **x**ylyl) electron transfer. Two impactful results were garnered from this analysis: 1) Entropic barriers controlled the adiabatic electron transfer kinetics; and 2) the free energy barriers were unaffected by the degree of electronic coupling within experimental uncertainty. The second result stands in contrast to the common expectation that enhanced electronic coupling lowers the free energy barrier. This analysis provides new insights into how electronic coupling influences the free energy and barriers for electron transfer reactions.

**Introduction**: Thermodynamic activation energies ultimately underlie the population and lifetimes of electron transfer products of light initiated reactions in molecular excited states as well as subsequent thermal reactions important for energy conversion, storage, and catalysis.[1-5] Despite a large body of research on the influence of donor-acceptor electronic coupling, $H_{DA}$, on inter- and intramolecular electron transfer kinetics, a comparative study of activation barriers for strongly and weakly coupled electron transfer reactions remain elusive. Weakly coupled (non-adiabatic) electron transfer reactions have been well-studied in proteins, bridged c, and in bimolecular reactions with great success.[6-10] In contrast, kinetic data for strongly coupled (adiabatic) intramolecular electron transfer reactions is rather limited, despite the existence of a sophisticated theoretical framework.[11-12] Thus, studies of structurally similar compounds that can be synthetically modified to exhibit strong or weak coupling present an opportunity to elucidate the influence of coupling on the enthalpic and entropic barriers for electron transfer.

A recently reported experimental approach has provided direct kinetic data on the influence of electronic coupling on the standard Gibbs free energy change, $\Delta G^o$, for some specific acceptor-bridge-donor (A-B-D) compounds that undergo intramolecular electron transfer on the nanosecond timescale.[13] Kinetic data for four A-B-D compounds based on a bis(tridentate)cyclometalated $Ru^{II}$ center covalently linked to a triphenylamine (TPA) through either a phenyl- or xylyl-thiophene bridge were utilized, **Scheme 1.** Compounds were anchored onto mesoporous $TiO_2$ thin films and, following light excitation, ultrafast electron injection into $TiO_2$ to led to the generation of $Ru^{III}$. As a result, a quasi-equilibrium between $Ru^{III/II}$ and $TPA^{+/0}$ was established and the kinetics of electron transfer between TPA and $Ru^{III}$ centers were measured.[13]

**Scheme 1: Redox equilibrium after excited state injection to TiO2.**

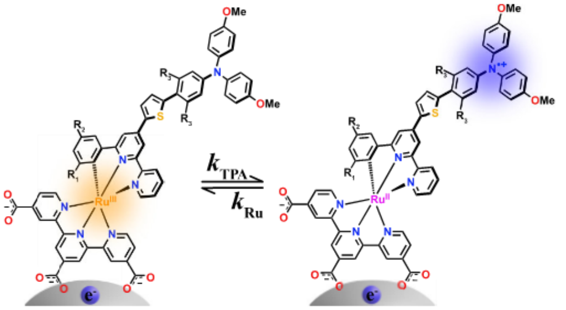

1: $R_1 = CF_3$, $R_2 = H$, **2**: $R_1 = H$, $R_2 = OCH_3$, **p/x**: $R_3 = H/CH_3$.

Equilibrium constants permitted the spectroscopic determination of the forward ($k_{TPA}$, TPA → $Ru^{III}$) and reverse ($k_{Ru}$, $Ru^{II} \rightarrow TPA^+$) electron transfer rate constants, Eq. 1. The driving force was controlled by substituents on the cyclometalating ligand to either inhibit ($\Delta G° > 0$ for 1) or promote ($\Delta G° < 0$ for 2) electron transfer from TPA to the $Ru^{III}$ center created after excited state injection into $TiO_2$.[14]

$$TiO_2|A\text{-}B\text{-}D + h\nu \rightarrow TiO_2(e^-)|A^+\text{-}B\text{-}D \rightleftharpoons TiO_2(e^-)|A\text{-}B\text{-}D^+ \qquad (1)$$

Indeed, prior analysis of the intervalence charge transfer bands in the one-electron oxidized forms of the compounds and revealed that the phenyl bridge promoted strong electronic coupling, $H_{DA}$, between the $Ru^{II}$ and

TPA centers and adiabatic ($H_{DA}$ > 1000 $cm^{-1}$) electron transfer while the methyl groups of the xylyl bridge disrupted conjugation that presumably resulted in non-adiabatic transfer, $H_{DA} \leq 150$ $cm^{-1}$.[15]

Here we report Eyring analysis of these data that provides the enthalpy and entropy of activation. For adiabatic electron transfer the barrier was predominantly determined by entropic factors rather than enthalpic contributions. Interestingly, the free energy barriers, $\Delta G^{\ddagger}$, were nearly the same for the adiabatic and non-adiabatic electron transfer. This was in stark contrast to an experimentalists assumption that enhanced coupling decreases the barrier for electron transfer.[16-17] The implication(s) of these experimental advances on electron transfer are discussed.

**Results**: The kinetic data used in this study was collected from a previous report that focused on the change in the free energy that accompanies electron transfer in the (non-)adiabatic limits without regard to the barriers. Thin films of $TiO_2$ were sensitized to visible light with compounds **1x**, **1p**, **2x**, and **2p** as surface coverages less than half the saturation value. The films were then immersed in 100 mM $LiClO_4/CH_3CN$ solutions. Pulsed laser excitation resulted in rapid ($k_{inj} > 10^8$ $s^{-1}$) excited-state electron injection and a quasi-equilibrium as described in **Scheme 1** and Eq. 1. Equilibration was quantified on a nanosecond and longer timescales over a 220-330 K range. Additional experimental details are provided in ref. 13.[13]

A van't Hoff analysis of the kinetic data for the compounds revealed that when the bridge orbitals promoted strong D-A electronic coupling the reaction was adiabatic, $\Delta H° = 0$ kJ $mol^{-1}$.[13] When the bridge was more insulating, the reaction was non-adiabatic, $\Delta H° \neq 0$ kJ $mol^{-1}$, **Figure 1** and **Table 1**. This analysis also indicated that when $H_{DA}$ > 1000 $cm^{-1}$, the driving force for the reaction, $|\Delta G°|$, was reduced in accordance with theoretical predictions.[13] Standard entropies for the reaction were also garnered from the intercept of the van't Hoff analysis. Interestingly, it was apparent that in the **p**-series a large entropy term, $|\Delta S°| = 18$ J $mol^{-1}$ $K^{-1}$ was noted in stark contrast to the **x**-series which had only a marginal standard entropy change, $|\Delta S°| = 2$ J $mol^{-1}$ $K^{-1}$.

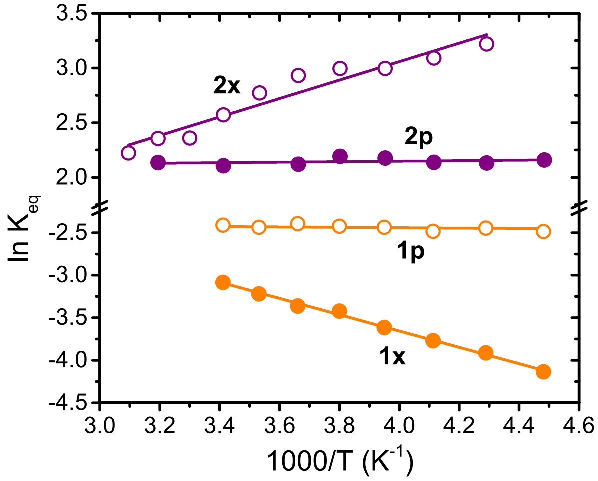

**Figure 1.** van't Hoff plot of electron transfer equilibrium constants for the studied compounds.[13]

**Table 1. Thermodynamic values for the indicated compounds in the redox equilibrium of Eq. 1.**

| Cmpd | ΔH°[a,b] | ΔS°[a,c] | ΔG°[b,d] | E° ($TPA^{+/0}$)[a] | E° ($Ru^{III/II}$)[a] |
|---|---|---|---|---|---|
| **1x** | +7.9 | +1.5 | +7.4 | 940 | 860 |
| **1p** | 0.0 | -18 | +5.9 | 940 | 860 |
| **2x** | -7.0 | -2.6 | -6.2 | 940 | 1010 |
| **2p** | 0.0 | +17 | -5.2 | 940 | 1030 |

[a]From Ref 13. [b]kJ mol$^{-1}$ [c]J mol$^{-1}$ K$^{-1}$ [d]T = 298 K. Note: thermodynamic values are defined relative to the $TPA^{+/0}$ redox couple.

Moving away from standard thermodynamic quantities, it is clear that the kinetic barriers will also provide insight following theoretical predictions: 1) the activation barriers are reduced in the presence of strong coupling, and 2) pre-exponential factors provide quantitative insights into reaction adiabaticity through the entropy of activation. Initial treatment of the temperature dependent data with the Arrhenius expression revealed very different pre-exponential factors between the xylyl- and phenyl-bridged compounds indicative of dynamical differences between the two mechanisms. Arrhenius analysis provided activation energies ($E_a$) and pre-exponential factors, ln(A), while Eyring analysis provided enthalpies ($\Delta H^{\ddagger}$), entropies ($\Delta S^{\ddagger}$) and Gibbs Free ($\Delta G^{\ddagger}$) energies of activation for the forward and reverse electron transfer reactions by Eq. 2.

$$\ln\left(\frac{k}{T}\right) = -\frac{\Delta H^{\ddagger}}{R}\frac{1}{T} + \frac{\Delta S^{\ddagger}}{R} + \ln\left(\frac{k_b}{h}\right) \tag{2}$$

where $k$ is the rate constant for a particular reaction, $k_b$ is the Boltzmann's constant, and $h$ is Planck's constant.

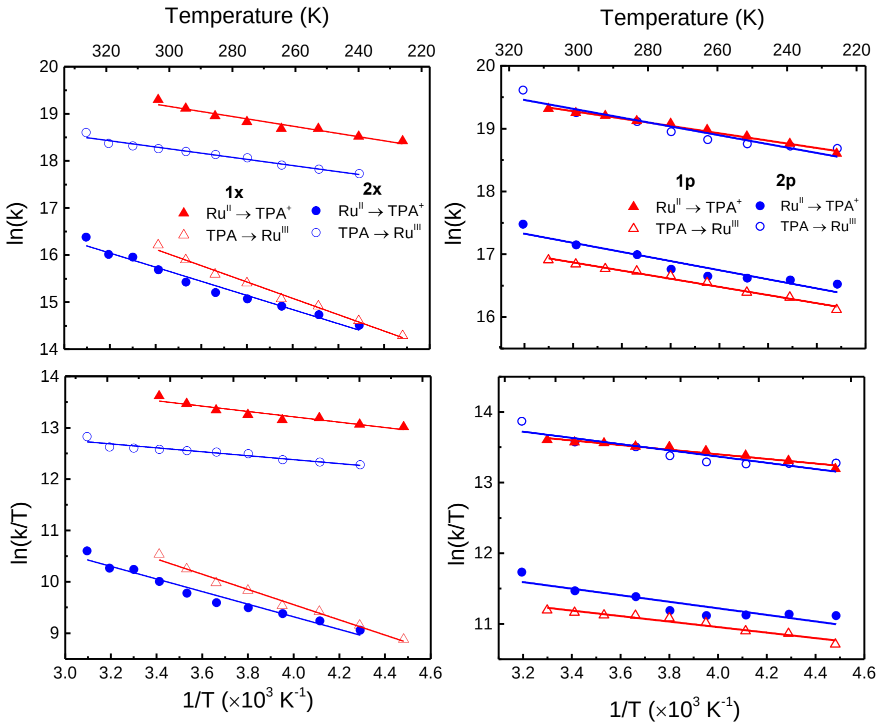

**Figure 2.** Arrhenius (top) and Eyring analysis (bottom) for the forward, TPA → $Ru^{III}$, $k_{TPA}$, (open shapes) and reverse, $Ru^{II}$ → $TPA^{+}$, $k_{Ru}$ (solid shapes) electron transfer rate constants for **1x**, **1p** (red triangles) and **2x**, **2p** (blue circles).

The overlaid solid lines demonstrate a good fit of the kinetic data to the Arrhenius and Eyring models, Figure 2. The extracted thermodynamic activation energies for each reaction are summarized in **Table 2**, and Arrhenius analysis results are included. For clarity, $k_{TPA}$ is the rate constant for the reaction TPA → $Ru^{III}$ while $k_{Ru}$ is the reverse process, $Ru^{II}$ → $TPA^{+}$. The driving force for the equilibrium reaction, as written, is uphill for **1x** and **1p** and downhill for **2x** and **2p**. That is to say that $k_{Ru}$ and $k_{TPA}$ can represent thermodynamically uphill or downhill reactions depending on the cyclometalating substituent.

**Table 2. Activation parameters for intramolecular electron transfer in the xylyl-bridged (nonadiabatic) and phenyl-bridged (adiabatic) compounds.**

| | **1x** | | **2x** | | **1p** | | **2p** | |
|---|---|---|---|---|---|---|---|---|
| | $k_{TPA}$ | $k_{Ru}$ | $k_{TPA}$ | $k_{Ru}$ | $k_{TPA}$ | $k_{Ru}$ | $k_{TPA}$ | $k_{Ru}$ |
| $\Delta H^{\ddagger a}$ | 12.3±0.6 | 4.3±0.6 | 3.2±0.3 | 10.2±0.7 | 3.2±0.2 | 2.7±0.2 | 3.6±0.7 | 3.8±0.7 |
| $\Delta S^{\ddagger b}$ | -70±2 | -70±2 | -80±3 | -80±1 | -94±2 | -75±2 | -70±3 | -89±1 |
| $\Delta G^{\ddagger a,c}$ | 32.8±0.9 | 25.3±0.8 | 27.0±0.5 | 34±1 | 30.4±0.3 | 25±0.2 | 24±1 | 30±1 |
| $E_a{}^a$ | 14.4±0.6 | 6.4±0.6 | 5.4±0.3 | 12.5±0.7 | 5.4±0.2 | 4.8±0.2 | 5.8±0.7 | 6.0±0.8 |
| ln(A) | 22.0±0.3 | 21.8±0.3 | 20.5±0.3 | 20.8±0.2 | 19.1±0.1 | 21.3±0.3 | 21.7±0.3 | 19.6±0.4 |

$^a$kJ mol$^{-1}$ $^b$J mol$^{-1}$ K$^{-1}$. $^c$T = 298 K.

**Discussion**: A van't Hoff analysis of the kinetic data afforded standard enthalpies and entropies for electron transfer between the $Ru^{III/II}$ and $TPA^{+/0}$ centers. For the phenyl-bridged compounds, the electron transfer reaction was adiabatic, $\Delta H^o = 0$ kJ mol$^{-1}$. Compounds that contained a xylyl-bridge, which disrupted conjugation, the reaction was non-adiabatic, $\Delta H^o \neq 0$ kJ mol$^{-1}$. The analysis also indicated that the Gibbs free energy, $\Delta G^o$, accompanying electron transfer was reduced in the phenyl bridged compounds relative to the weakly coupled xylyl-bridged compounds, *i.e.* $|\Delta G^o_{ad}| < |\Delta G^o|$. Further, the standard entropy change $\Delta S^o$ was substantially different between the two kinetic limits. Spectroelectrochemical experiments and interfacial electron transfer recombination kinetics indicated two discrete redox reactions to either $Ru^{III/II}$ or $TPA^{+/0}$ regardless of the bridge structure.[15, 18] This observation implies that, despite strong electronic coupling in the phenyl-bridged compounds, $H_{DA} > 1000$ cm$^{-1}$, the redox chemistry was localized and discrete minima for reactants and products exist. Hence, entropic and enthalpic *barriers* for electron transfer were measurable.[18]

Many previously reported models for electron transfer partition the entropy and enthalpy of activation into a pre-exponential factor and a Boltzmann-weighted exponential term, respectively. The magnitude of the activation entropy is further dependent on the adiabaticity of the reaction and, in some cases, the kinetic model applied. As such, we first consider the common models of Eyring and Marcus and account for the influence of coupling on the pre-exponential factors. We then apply these models to the kinetic data reported herein to quantify entropies, enthalpies, and free energies of activation for adiabatic and non-adiabatic electron transfer. Determination of $H_{DA}$ is briefly addressed and calculations of the total reorganization energy, $\lambda$, are presented. Finally, the entropic barriers are discussed in the context of vibrational entropy and solvent dynamical effects on the electron transfer reactions.

**Pre-exponential factors**: It is critical to establish criteria for appropriate use of pre-exponential factors. Within this section, such criteria is presented and discussed in context of the studied compounds. Arrhenius analysis, $k_{\mathrm{et}} = \mathrm{A}\exp(-\mathrm{E_a}/\mathrm{k_bT})$, takes the ratio of forward and reverse pre-exponential factors to provide information on the standard entropy change, ΔS°, through Eq. 3.**[19]**

$$\frac{A_{TPA}}{A_{Ru}} = \frac{\exp(S_{TPA}/k_b)}{\exp(S_{Ru}/k_b)} = \exp\left(\frac{\Delta S^o}{k_b}\right) \tag{3}$$

Where $\mathrm{A_{TPA}}$ and $\mathrm{A_{Ru}}$ are the pre-exponential factors for $\mathrm{Ru^{II}} \rightarrow \mathrm{TPA^+}$ and $\mathrm{TPA} \rightarrow \mathrm{Ru^{III}}$ electron transfer reactions. In this case, however, no explicit expression is written for $\Delta S^‡$. Analysis of the pre-exponential factors yielded standard entropies that were in good agreement with the results of the van't Hoff treatment. Values extracted from the van't Hoff analysis are given in Table 1 and those from Arrhenius analysis in Table 3.

In transition state theory, the pre-exponential factor yields $\Delta S^‡$ directly as it is temperature independent, Eq. 4. Here, $\kappa_{\mathrm{el}}$ is the transmission coefficient, T is the temperature, and $\Delta G^‡ = \Delta H^‡ - T\Delta S^‡$. Notably $\mathrm{H_{DA}}$ and λ do not appear in the rate expression explicitly. When $\kappa_{\mathrm{el}} = 1$ this approach is elegant and applied easily provided that the reaction is truly adiabatic.

$$k_{et} = \kappa_{el}\frac{k_bT}{h}e^{\left(-\frac{\Delta G^‡}{k_bT}\right)} = \kappa_{el}\frac{k_bT}{h}e^{\left(-\frac{\Delta H^‡}{k_bT}+\frac{\Delta S^‡}{k_b}\right)} \tag{4}$$

Hence, a subtle yet important detail is properly accounting for non-adiabaticity.[20-21] Adiabaticity has previously been accounted for through the Landau-Zener electronic transmission coefficient, $\kappa_{\mathrm{el}}$, calculated through Eq. 5, which uses electronic, $\nu_{\mathrm{el}}$, and nuclear, $\nu_{\mathrm{n}}$, frequency factors[22]

$$\kappa_{el} = \frac{2[1-\exp(\nu_{el}/2\nu_n)]}{2-\exp(\nu_{el}/2\nu_n)} = \exp\left(\frac{\Delta S_{el}^‡}{k_b}\right) \tag{5}$$

with $\nu_{\mathrm{el}}$ given by Eq. 6.

$$\nu_{el} = \frac{2\pi}{\hbar}\frac{{H_{DA}}^2}{\sqrt{\lambda k_bT}} \tag{6}$$

Where $\nu_{\mathrm{n}}$ is a vibrational frequency taken as $k_b\mathrm{T}/h$, as in transition state theory, or in some cases as high frequency modes if they dominate the reaction coordinate, and λ is the reorganization energy.[23] This factor represents the probability of the reaction proceeding from the reactant surface, through the transition state, and ultimately to the product potential energy surface. Generally, when $\nu_{\mathrm{el}} >> 2\nu_{\mathrm{n}}$, the reaction is adiabatic, $\kappa_{\mathrm{el}} = 1$, and rate limited by $\nu_{\mathrm{n}}$. For $\lambda = 1$ eV and $\nu_{\mathrm{n}} = \mathrm{k_bT/h}$, adiabaticity is achieved at $\mathrm{H_{DA}} = 300\ \mathrm{cm^{-1}}$ ($(3/2)\mathrm{k_bT}$), that is $\kappa_{\mathrm{el}} > 0.9$. Of course, the additional entropic contributions from $\kappa_{\mathrm{el}}$ arise as a result of the limited orbital mixing, i.e. *delocalization*, between the redox centers which necessitates a particular electronic structure to be achieved in order to undergo electron transfer.

Marcus and Sutin have derived Eq. 7 which partitions the measured activation entropy into a sum of nuclear and electronic entropies. In other words, $\Delta S^‡$ is a sum of nuclear and electronic entropy contributions.[5, 21]

$$\Delta S^{\ddagger} = \Delta S_n^{\ddagger} + \Delta S_{el}^{\ddagger} = \Delta S_n^{\ddagger} + k_b \ln(\kappa_{el}) \qquad (7)$$

where $\Delta S^{\ddagger}_{n}$ is the inherent nuclear entropy arising from solvent and vibrational motion and $\Delta S^{\ddagger}_{el}$ is the entropy arising from the reaction (non-)adiabaticity. In principle, calculation of $\kappa_{el}$ subsequently allows one to correct for non-adiabaticity. Electronic factors contribute to $\Delta S^{\ddagger}$ when $\kappa_{el} \neq 1$. Hence, the minimum entropic barrier is realized when $\kappa_{el} = 1$ and the reaction is adiabatic. On the other hand, when $\kappa_{el} < 0.5$, the factor $k_b\ln(\kappa_{el})$ can become significant, on the order of -6 J $mol^{-1}$ $K^{-1}$.

Turning now to Marcus theory, a continuum description for the influence of electronic coupling on the rate of electron transfer is given by Eq. 8.[24]

$$k_{ET} = \frac{2\pi}{\hbar} \frac{|{H_{DA}}^2|}{\sqrt{4\pi\lambda k_b T}} \left[\frac{1}{1+\kappa_A}\right] \exp\left(\frac{\Delta G^{\ddagger}}{k_b T}\right) \qquad (8)$$

Where $\kappa_A$ is the Rips-Jortner adiabaticity factor given by eq. 9[25]

$$\kappa_A = \frac{4\pi\tau_L {H_{DA}}^2}{\hbar\lambda} \qquad (9)$$

Here, $\tau_L$, is the longitudinal solvent reorientation lifetime which is a constant for a given solvent. This adiabaticity factor, $\kappa_A$, indicates the extent to which solvent motion influences a reaction rate. When $\kappa_A >> 1$, the electron transfer rate expression becomes independent of $H_{DA}$, Eq. 10,[26]

$$k_{ET} = \frac{1}{\tau_L} \sqrt{\frac{\lambda}{16\pi k_b T}} \exp\left(-\frac{\Delta G^{\ddagger}}{k_b T}\right) \qquad (10)$$

and the adiabatic reaction is defined as solvent-controlled.[27] Solvent dipole reorientation is slower than low-frequency vibrational modes, ~200 $cm^{-1}$, and becomes the rate limiting factor for the reaction discussed in more detail below.[28]

A final point lies in the temperature dependent rate constants. Prior to linear regression analysis, rate constants are temperature-normalized to account for the temperature factor within the pre-exponential term. As a result, temperature factors in Eyring, ln(k/T), and Marcus, $\ln(kT^{1/2})$, analysis *vs.* 1/T yield different slopes (and intercepts). The general relationship between Marcus and Eyring models is given by Eq. 11

$$\Delta H_M^{\ddagger} = \Delta H_E^{\ddagger} + \frac{3}{2} k_b T \qquad (11)$$

where $\Delta H^{\ddagger}_{M}$ and $\Delta H^{\ddagger}_{E}$ are the Marcus and Eyring enthalpies of activation, respectively, provided they are on the order of $k_b$T as is the present case. The relationship between the two kinetic models arises as a result of the Gibbs-Helmholtz relation. A derivation is presented in the SI analogous to the well-known relationship between Eyring and Arrhenius analysis where $E_a = \Delta H^{\ddagger}_{E} - k_b T$.[29] Importantly, the total Gibbs Free energy of activation, $\Delta G^{\ddagger}$, were model independent. When $\kappa_A >> 1$, the maximum pre-exponential factor for a solvent-controlled adiabatic reaction, Eq. 10, is predicted to be $7\times10^{13}$ $s^{-1}$ with $\lambda = 1$ eV in acetonitrile. Under Eyring analysis, the maximum is $k_b/h = 2\times10^{10}$ $s^{-1}$ – a three order of magnitude difference that is accounted for by the difference in activation enthalpies and temperature factors.

In summary, guidelines for appropriate use of pre-exponential factors from Eyring and Marcus analysis were presented. Both models have a continuum expression that link non-adiabatic and adiabatic electron transfer reactions with known values of $H_{DA,}$ $\lambda$, $\nu_n$, and $\tau_L$. The intercepts from these data, as a result, properly account for the influence of non-adiabaticity on $\Delta S^{\ddagger}$. Differences in $\Delta H^{\ddagger}$ values between the models are accounted for by the Gibbs-Helmholtz relationship with the important realization that the free energy of activation, $\Delta G^{\ddagger}{}_{,}$ is conserved. This discussion allows for some comment on the physical manifestation of reaction adiabaticity. Adiabatic Marcus theory indicates that the reaction is limited by solvent motion, seen in the pre-exponential factor. However, the pre-exponential factor in the Eyring model arises from the vibrational and/or rotational partition functions resulting in a frequency factor of $k_bT/h$. In the following sections, the experimental data are analyzed under the Eyring formalism. Emphasis is placed on differentiating the solvent-controlled adiabatic reactions for the phenyl-bridged compounds from the non-adiabatic reactions for the xylyl-bridged compounds. Results of the kinetic analysis which yield the entropies, enthalpies and free energies of activation are discussed.

**Entropy of Activation:** Electron transfer reactions for the xylyl-bridged compounds were shown to be non-adiabatic by the results of the van't Hoff analysis. In addition, the mixed-valent form of the xylyl-bridged compounds did not display significant optical data indicative of low-energy intervalence charge transfer bands, concomitant with the weak coupling and non-adiabatic electron transfer. The degree of coupling is, however, uncertain with an upper-limit of 150 $cm^{-1}$ likely under the experimental conditions used. Assuming $\lambda = 1$ eV (see Reorganization Energy for a detailed discussion) and $\nu_n = k_bT/h$, $\kappa_{el} = 0.56$ (from Eq. 5) which an upper estimate at 298 K. This affords an electronic entropy contribution of $\Delta S^{\ddagger}_{el} = -5$ J $mol^{-1}$ $K^{-1}$. This indicates a reasonable value for electronic coupling of ~100 $cm^{-1}$, which corresponds to $\kappa_{el} = 0.32$ and $\Delta S^{\ddagger}_{el} = -10$ J $mol^{-1}$ $K^{-1}$, doubling the electronic entropy contribution. Determination of the electronic entropy allowed the measured entropy of activation $\Delta S^{\ddagger}$ to be partitioned into the electronic and nuclear components for the forward and reverse reaction in the redox equilibrium.

Assuming $\lambda = 1$ eV with $H_{DA} = 1000$ $cm^{-1}{}_{,}$ using Eq. 5 resulted in $\kappa_{el} = 1$ for the phenyl-bridged compounds. As a result, entropic factors measured arose solely from nuclear contributions, $\Delta S^{\ddagger}_{n}$, as $\Delta S^{\ddagger}_{el} = 0$ J $mol^{-1}$ $K^{-1}$. Inclusion of the non-adiabatic correction term allows the entropic barriers to be correctly distinguished between non-adiabatic and adiabatic electron transfer mechanisms. The standard entropy change, the total activation entropy and the deconvoluted nuclear and electronic entropy terms are presented in Table 3.

**Table 3**. Standard and thermodynamic activation entropies for electron transfer.

| | **1x** | | **1p** | | **2x** | | **2p** | |
|---|---|---|---|---|---|---|---|---|
| Rxn | $k_{TPA}$ | $k_{Ru}$ | $k_{TPA}$ | $k_{Ru}$ | $k_{TPA}$ | $k_{Ru}$ | $k_{TPA}$ | $k_{Ru}$ |
| $\Delta S^{oa}$ | 0 | | -18 | | +2 | | +17 | |
| $\Delta S^{\ddagger a,c}$ | -70 | -70 | -93 | -75 | -78 | -80 | -73 | -90 |
| $\Delta S^{\ddagger}{}_{el}{}^{a,b}$ | -10 | -10 | 0 | 0 | -10 | -10 | 0 | 0 |
| $\Delta S^{\ddagger}{}_{n}{}^{a,c}$ | -60 | -60 | -93 | -75 | -68 | -70 | -73 | -90 |

[a] J $mol^{-1}$ $K^{-1}$. [b] From equation 6. [c] Using experimental data with from equation 2. [d] From equation 8.

Of particular interest in **Table 3** are the values for $\Delta S^{\ddagger}_{el}$, and $\Delta S^{\ddagger}_{n}$. The xylyl-bridged compounds have smaller $\Delta S^{\ddagger}_{n}$ contributions to $\Delta S^{\ddagger}$ than do the phenyl-bridged compounds. Further, an interesting phenomenon was observed by comparing the nuclear entropic barriers for the endergonic ($k_{TPA}$ for **1** and $k_{Ru}$ for **2**) and exergonic reactions of the phenyl-bridged compounds. Namely that the difference between the nuclear barriers, $|\Delta\Delta S^{\ddagger}_{n}| = \sim 20$ J mol$^{-1}$ K$^{-1}$, is likely also the origin of the large values for $\Delta S^{o}$ garnered from Arrhenius and van't Hoff analysis. Taken together, the results of the pre-exponential factor analysis support two conclusions: 1) Accounting for adiabaticity properly differentiated betweenthe entropic barriers for adiabatic and non-adiabatic electron transfer, and 2) The barrier of the uphill reaction in the adiabatic limit is ~20 J mol$^{-1}$ K$^{-1}$ larger relative to the downhill process as was reflected through $\Delta S^{o}$. These results demonstrate that the product is entropically stabilized relative to the reactant when electronic coupling is present. This analysis, however, does not characterize the molecular origin of these barriers which is discussed later.

**Enthalpy of Activation**: For compounds **1x** and **2x**, the thermodynamically uphill process displayed enthalpic barriers ~3 times larger than the corresponding downhill process (*e.g.* $\Delta H^{\ddagger} = 12.3$ kJ mol$^{-1}$ and 4.3 kJ mol$^{-1}$ for $k_{TPA}$ and $k_{Ru}$ respectively). Because the reactions of interest occur thermally and are intramolecular, small enthalpic barriers are wholly consistent with a through bond hole-transfer mechanism where no covalent bonds are broken.[7, 30-32] Differences in $\Delta H^{\ddagger}$ between the xylyl-bridged compounds can be rationalized by the influence of either electron withdrawing ($-CF_3$) or donating ($-OCH_3$) substituents. These inductive effects modulate the energetic proximity of the bridge orbitals to either the TPA (**1x**) or Ru$^{II}$ center (**2x**) causing electron transfer to Ru$^{III}$ to be downhill or uphill, relative to the TPA reduction potential.[33] When Ru$^{II}$ was electrochemically oxidized prior to TPA, as in **1x** and **1p**, an inductive influence of the oxidized metal center resulted in an increased energy of the bridge-centered orbitals thus leading to a larger barrier.

Enthalpic barriers for the phenyl-bridged compounds were surprisingly similar for the forward and reverse adiabatic reactions. For phenyl-bridged compounds the barriers in either the forward or reverse direction were, within experimental error, the same (*e.g.* $\Delta H^{\ddagger} = 3.0\pm0.3$ and $3.7\pm0.1$ kJ mol$^{-1}$). When $H_{DA} > 1000$ cm$^{-1}$, the data indicate that $\Delta H^{\ddagger}$ for the reverse reaction was greatly reduced, $\Delta H^{\ddagger} = 3$ kJ mol$^{-1}$, relative to the non-adiabatic compounds, $\Delta H^{\ddagger} = 11$ kJ mol$^{-1}$. On the other hand, the downhill process barrier remained essentially unchanged, $\Delta H^{\ddagger} \sim 3\text{-}4$ kJ mol$^{-1}$. Interestingly, the barriers for the forward and reverse reactions are very similar to the longitudinal relaxation of $CH_3CN$, with $\Delta H_L^{\ddagger} = 4.9$ kJ mol$^{-1}$.[34] In the adiabatic limit, the transient kinetics were similarly temperature dependent, **Table 2** and a standard enthalpy change was not observed for redox equilibrium, $\Delta H° = 0$ kJ mol$^{-1}$. As a result the equilibrium constant, $K_{eq}$, was demonstrated by the van't Hoff analysis to be temperature independent, **Figure 1**. An important conclusion from combining the results of the Eyring and van't Hoff analyses is that the equilibrium concentrations of Ru$^{III}$ and TPA$^{+}$ were entirely dictated by enthalpy for the xylyl-bridged compounds while the nuclear entropy was the dominant factor for the phenyl-bridged compounds.

**Free energy of Activation**: Evaluating the intercepts and slopes from the Eyring analysis yielded values of $\Delta S^\ddagger$ and $\Delta H^\ddagger$. From those results, it is evident that the enthalpic barriers do not contribute significantly to the total free energy barrier, $\Delta G^\ddagger = \Delta H^\ddagger - T\Delta S^\ddagger$, at 298K. The main result arising from calculation of $\Delta G^\ddagger$ is that the free energy barriers were independent of the electronic coupling. For the uphill reactions $\Delta G^\ddagger = 30$ kJ mol$^{-1}$ across the series while for the downhill reaction $\Delta G^\ddagger = 25$ kJ mol$^{-1}$. Indeed, the independence of the free energy barriers with respect to (non-)adiabaticity was surprising. Theory predicts, and some experiments have demonstrated, that a decrease in $\Delta G^o$ and $\Delta G^\ddagger$ is expected with increased $H_{DA}$ by virtue of the energy splitting in the transition state, **Scheme 2**.[11, 35-37] The scheme also demonstrates the theoretical expectation of decreases in the activation energy in the transition state (left panel) as the electronic coupling increases. It is recognized that one-dimensional reaction coordinates are likely too simplistic to capture the 3N-6 vibrational and/or solvent modes. The approach does, however, provide a great deal of insight into how potential energy surfaces trend with factors such as $\lambda$, $\Delta G^o$, and $H_{DA}$. At a cursory level, the schematic surfaces indicate that $\Delta G^\ddagger$ decreases linearly with $H_{DA}$. Additionally, the splitting between the upper and lower surfaces is $2H_{DA}$ for $\Delta G^o = 0$ eV, and to a first approximation that holds for the compounds used in this study, $\Delta G^0 < 100$ mV. Higher order algebraic expressions for $\lambda$, $\Delta G^o$, and $H_{DA}$ are known.[17]

**Scheme 2. Two-dimensional potential energy surfaces for asymmetric electron transfer.**

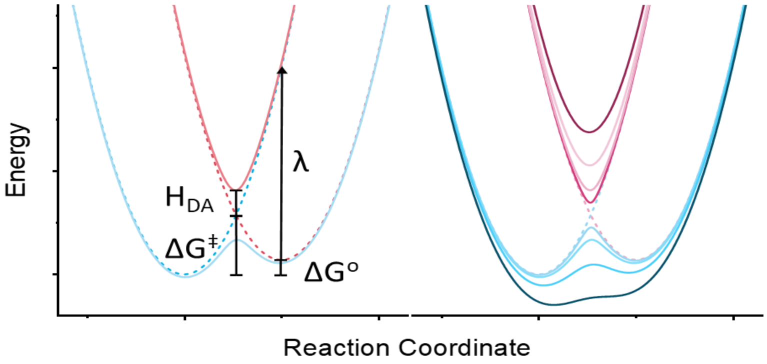

Thus, with the large electronic coupling between the Ru$^{II}$ and TPA centers the initial expectation is that $\Delta G^\ddagger$ would decrease and $k_{ET}$ would approach a maximum value. The maximum rate for a barrierless reaction under the Eyring formalism is $\nu_n = k_bT/h$, while for adiabatic Marcus theory the solvent modes ultimately dominate the reaction, $1/\tau_L \sim 5\times10^{12}$ s$^{-1}$ (for a given $\lambda$), which is the kinetic speed limit. However, the experimentally determined values were ~$10^4$ times slower at all temperatures investigated, even when the decrease in $\Delta G^o$ is accounted for. Clearly, the free energy barrier still must dictate the kinetics.

Deconvolution of $\Delta G^\ddagger$ into its enthalpic and entropic components indicates that $\Delta H^\ddagger$ comprises 10-40% of $\Delta G^\ddagger$ for the xylyl-bridged compounds. By contrast for the phenyl bridged compounds, $\Delta H^\ddagger$ is just 10-15% of $\Delta G^\ddagger$. More specifically, for all compounds studied herein, $|T\Delta S^\ddagger|$ is >17 kJ mol$^{-1}$ on average at 298K, similar to values measured for bimolecular electron transfer in $CH_3CN$.[8] Careful analysis revealed that electronic entropy did not influence the barriers for the phenyl-bridged compounds, while the opposite was observed for the xylyl-bridged compounds: non-adiabaticity effectively increased the entropic barrier. From Table 3, it is clear that the nuclear entropy of activation is critical in explaining the differences between the two mechanisms. Lastly, the observation that the free energy barrier was independent of the vastly different electronic coupling elements was unexpected. In order to compare the results directly with electron transfer models described above, we turn now to calculations of the rate constants and reorganization energies for the adiabatic and non-adiabatic regimes.

***A priori* rate calculations**: Theoretical expectations allow for rate constants for electron transfer to be predicted using the previously presented Marcus theory continuum expression, Eq. 8, using only spectroscopic and electrochemical data with an assumed reorganization energy of $\lambda = 1$ eV. Because electronic coupling through the xylyl-bridge was taken as 150 cm$^{1}$, and $\tau_L = 0.2\times10^{-12}$ s$^{-1}$ for neat $CH_3CN$, the Jortner adiabaticity parameter begins to contribute, at room temperature $\kappa_A = 1.3$. For example, Figure 3 shows calculated electron transfer rate constants using Eqs. 8 and 10 as a function of electronic coupling when $\Delta G^{\ddagger} = 24$ kJ mol$^{-1}$. These simulated data demonstrate the parabolic dependence of the rate constants when $\kappa_A = 0$. More interesting is the situation when $\kappa_A > 0$. Here, an initially non-adiabatic rate constant accelerates with $H_{DA}^2$ for $0 < H_{DA} < 100$ cm$^{-1}$, followed by a transition into a mixed (non-)adiabatic regime, $100 < H_{DA} < 350$ cm$^{-1}$, after which the rate constant becomes coupling-independent, $H_{DA} > 350$ cm$^{-1}$ and $\kappa_A >> 1$. The so-called 'speed limit' is calculated from Eq. 10, and is shown as the blue dashed line in Figure 3.

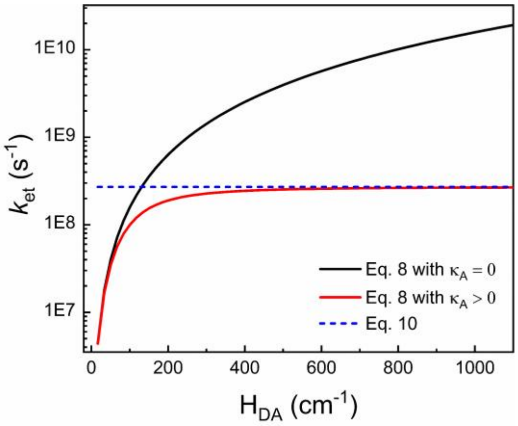

**Figure 3.** Electron transfer rates as a function of electronic coupling for a purely non-adiabatic reaction (Eq. 8, $\kappa_A = 0$, black), a non-adiabatic reaction with the adiabaticity parameter (Eq. 8, $\kappa_A > 0$, red) and a solvent-controlled adiabatic reaction (Eq. 10, dashed blue line). Parameters used in these calculations: T = 298 K, $\lambda = 1$ eV, $\tau_L = 0.2$ ps, $\Delta G^{\ddagger} = 24$ kJ mol$^{-1}$.

Thus, Eq. 8 is applicable to the xylyl-bridged compounds. Indeed, calculated rate constants for **1x** and **2x** show good agreement with experiment. If $\kappa_A$ is ignored for the non-adiabatic electron transfer reactions, the pre-exponential term was indeed larger than would be allowed by $\tau_L$.

Moving now to the phenyl-bridged compounds, $\kappa_A = 53$ which places the kinetics firmly in the limit $\kappa_A >> 1$, and the reaction is adiabatic (see SI, Table S2). In this limit, the electron transfer rate was expected to be independent of the coupling and limited instead by the frequency with which the reactant approaches the transition state which depends on properties of the solvent.[38-39] As a result, eq. 10 becomes solely applicable. If the adiabaticity factor were ignored, predicted rate constants were found to differ by factors of 40-100 from experiment.[25, 27] The pre-exponential term in Eq. 5 represents the kinetic speed limit for electron transfer between strongly coupled redox centers with $k_{ET}$ governed by solvent reorientational motion, $1/\tau_L$, ($5\times10^{12}$ $s^{-1}$ for $CH_3CN$).[40] Equations 8 and 10 accurately reproduced experimental rate constants to within factors of 1 to 3. Selected rate constants are presented in **Table 4**, with the remainder of the rate constants as well as the calculation methodology presented in the SI.

**Table 4. Calculated and observed rate constants of intramolecular electron transfer at 293 K.**

| Rate ($x10^7$ $s^{-1}$) | | **1x**[a] | **2x**[a] | **1p**[b] | **2p**[b] |
|---|---|---|---|---|---|
| $k_{TPA}$ | *Obs.*[c] | 0.45 | 8.5 | 2.1 | 23 |
| | *Calc.*[d] | 0.35 | 4.5 | 1.4 | 22 |
| $k_{Ru}$ | *Obs.*[c] | 1.0 | .65 | 23 | 2.8 |
| | *Calc.*[d] | 0.94 | .25 | 18 | 1.8 |

[a]Using Eq. 8. [b]Using Eq. 10. [c]Experimentally determined. [d]Calculated from Eqs. 8 or 10.

**Reorganization Energy**: The total reorganization energy was calculated by Eq. 12, which relates the activation free energies to the standard free energy and reorganization energy for an electron transfer reaction.

$$\Delta G^{\ddagger} = \frac{\left(\Delta G^{\circ} + \lambda\right)^2}{4\lambda} \tag{12}$$

By definition, the reorganization energy corresponds to the vertical energy difference between the reactants and products potential energy surfaces, **Scheme 2**.[17] The total reorganization energy, λ, is generally partitioned into the outer-sphere ($\lambda_o$) and inner-sphere ($\lambda_i$) reorganization energies for solvent reorganization and bond length changes, respectively, so $\lambda = \lambda_o + \lambda_i$. Temperature dependent values of $\Delta G^0$ and $\Delta G^{\ddagger}$ provided the necessary quantities to calculate λ. Solutions to Eq. 12 provided two values, λ = 0.004 eV or 1.2 eV. It is clear that the larger of the two values is a more physically appropriate number as the intramolecular reactions are well within the Marcus normal region and are certainly not activationless. Apart from Eq. 12, a value for λ at room temperature has been determined by three additional methods: the dielectric continuum approximation, spectroscopic data on intervalence charge transfer transitions, and generalized Mulliken-Hush theory.

For brevity and clarity, the dielectric continuum estimation is presented in the SI and predicts λ ~ 0.9 eV, close to the standard literature value for electron transfer reactions in acetonitrile.[41] Note that the dielectric continuum estimation provides a value only for $\lambda_o$. A key value for calculation of the reorganization energy is the geometric distance, $r_{DA}$, between the Ru and TPA centers which was taken as $r_{DA}$ = 14 Å from density functional theory calculations. It is acknowledged that the geometric distance is an upper-limit for the true charge transfer distance. Analysis of intervalence charge transfer optical data for the phenyl-bridged compounds that allowed for $H_{DA}$ to be calculated utilize band shape parameters that ultimately relate to the total reorganization energy through Eq. 13,

$$\lambda = \frac{(\Delta\nu_{1/2})^2}{16\ln(2)\mathrm{RT}} \tag{13}$$

where $\Delta\nu_{1/2}$ is the full-width at half-maximum of the intervalence charge transfer band.[42-43] This analysis gave $\lambda$ = 0.9-1.1 eV with $\Delta\nu_{1/2}$ = 4100-4500 $cm^{-1}$.[15] Generalized Mulliken-Hush theory, which accounts for delocalization-induced reduction of $r_{DA}$ from the geometric distances uses computationally calculated changes in dipole moments. This analysis provided $\lambda$ = 0.7 eV.[13, 44] These three independent measures of the reorganization energy are in reasonably good agreement with each other and are similar to commonly accepted values of for electron transfer in transition metal compounds in $CH_3CN$.[45-47] This supports the value of 1 eV used in the previous calculations.

The inner-sphere contribution is often assumed to be zero as $Ru^{II}$ polypyridyl complexes display the experimentally indistinguishable Ru-N bond length distortions between the 3+ and 2+ formal oxidation states.[48] It is acknowledged that the covalent cyclometalating bond is unaccounted for under this assumption and literature searches for crystal structure data, to the best of our knowledge, are notably absent. Additionally, $\lambda_i$ for a series of substituted $TPA^{+/0}$ redox couples have been predicted to range from 0.1 and 0.25 eV.[49] Thus, the calculations of $\lambda$ are reasonable even when including a non-zero inner-sphere reorganization.

**Standard Thermodynamics:** A critical advantage in addressing the influence of electronic coupling on the activation and reorganization energies for the compounds lies in the inherent energetic asymmetry of the $Ru^{III/II}$ and $TPA^{+/0}$ redox centers, which have non-zero standard thermodynamic quantities. In self-exchange model systems, $\Delta G^\circ$ = 0 kJ $mol^{-1}$ so moving between nonadiabatic to adiabatic regimes results in equal stabilization of the product and reactant surfaces relative to one another and critical details are lost.[17] Thus, revisiting the standard thermodynamic quantities may provide some insight into the apparent thermodynamic activation parameters. Standard entropies for the xylyl-bridged compounds were $\Delta S^\circ \approx -2 \pm 2$ J $mol^{-1}$ $K^{-1}$, a negligible entropic contribution, with a predominant enthalpic incentive of +7 and -8 kJ $mol^{-1}$. The opposite was true in the adiabatic limit due to the apparent thermodynamically favorable entropy changes, $\Delta S^\circ = +18 \pm 2$ J $mol^{-1}$ $K^{-1}$ and a negligible enthalpic contribution. While the necessary extrapolation to infinite temperature can raise uncertainty in the physical nature of the van't Hoff model, this analysis nevertheless provides self-consistent values to those extracted from the Eyring model and are independent of reaction adiabaticity over the range of temperatures investigated. After accounting for electronic entropy, a direct comparison between the non-adiabatic and adiabatic barriers implicates that electronic coupling manifests as nuclear entropy which is the origin of the stabilizing entropic incentive. Ultimately, the larger entropy term in the adiabatic limit result in the similar values of $\Delta G^\ddagger$. However, the molecular origin of the nuclear entropy is not easily distinguishable.

**Origin of Entropic Barriers**: With the underlying activation barriers resolved and reaction adiabaticity properly accounted for the following question arises: what do the standard thermodynamic quantities ultimately indicate regarding adiabatic and nonadiabatic electron transfer? At a minimum, the large change in $\Delta S^o$ between the xylyl- and phenyl-bridged compounds cannot adequately be explained by electronic coupling effects. Enthalpic barriers, while partially indicative of $H_{DA}$ contributions, do not satisfactorily characterize the molecular origin, either. Comparison of the kinetic and thermodynamic data herein with prior work is helpful in defining a reasonable molecular picture. Results from this study indicated that entropic contributions to electron transfer rate constants manifest as 'nuclear' entropic terms, $\Delta S^{\ddagger}{}_{n}$, when in an adiabatic regime. A logical starting point for discussion is the structure of the transition state.

For non-adiabatic processes the transition state structure is often invoked as the main contributor to the entropy of activation, $\Delta S^{\ddagger}$.[50] Measurement and interpretation of such barriers has been performed on Diels-Alder or condensation-type exemplar reactions, and many indicated that the loss of translational and rotational degrees of freedom are the sources of $\Delta S^{\ddagger}$.[51-52] Compounds anchored to $TiO_2$ are assumed to be stationary. As such, a covalent and rigid bridge likely minimizes translational and rotational motion. Such conclusions are justifiable through comparison with enzymatic catalysis, where a bound substrate removes translation and rotational degrees of freedom and the entropic contributions have been 'paid' prior to any chemistry occurring.[53-54]

Beyond rotational and translation motion, *inter*molecular electron transfer reactions between neighboring $Ru^{II}$-B-TPA compounds could have occurred on a similar timescale with unusual entropic factors.[55] However, in this study intermolecular electron transfer was minimal in these studies that were performed below a critical percolation threshold – inhibiting lateral electron transfer pathways.[56-57] Solvent structure or polarity also influences rates of electron transfer at a surface. The carboxylate derivatized compounds anchored onto $TiO_2$ are nearly insoluble in acetonitrile and may give rise to solvent exclusion effects.[58-59] Thus one may expect the reorganization energy to vary. Previous work has demonstrated that intermolecular and/or intramolecular reactions for the compounds anchored onto a metal oxide surface are similar to those reported in acetonitrile fluid solution.[46-47] Finally, electric fields generated by electrons injected into $TiO_2$ are known to transiently induce a Stark-like effect on the ground state absorption spectra of compounds anchored onto the surface.[60-61] Charge screening by 100 mM $Li^+$ efficiently dampens the field and thus effects are expected to be minimal for the pendant TPA located nearly 20 Å away from the surface.[62] Furthermore, calculation of equilibrium constants from electrochemical data for the xylyl-bridged compounds indicated that $\Delta G^0$ did not change. In turn, the electric field effect created by injected electrons did not significantly perturb the redox equilibrium.

Finally, significant literature precedent exists for vibrational entropic factors in transition metal complexes of Fe, Co, and Ru undergoing bimolecular (proton-coupled) electron transfer reactions. For Ru-based reactants, $\Delta S^o = 25$ J mol$^{-1}$ K$^{-1}$. The origin of the barriers were ascribed to low-frequency vibrational modes, $E_{vib} \leq 200$ cm$^{-1}$. Careful control experiments ruled out solvent effects as well as translational and rotational entropy.[63,64] Indeed, the importance of vibrational factors have been experimentally demonstrated for many transition metal half reactions which displayed large positive standard entropy changes and is garnered from summation over all available modes.[65] Considering that for the xylyl-bridged compounds $\Delta S^o \sim 0$ J mol$^{-1}$ K$^{-1}$ and implies that, even if vibrational frequencies do change, the net effect is zero.

More applicable to the adiabatic limit are bridged mixed-valent compounds with positive standard entropies. The origin of these entropic factors was a result of *decreases* in vibrational frequencies resulting from charge delocalization through the intervening bridge and charge balance between redox centers.[66] In this limit, solvent reorientation occurs over a larger volume which necessitates a more ordered solvation shell around the compound, effectively reducing the number of available solvent configurational microstates.[**67-68**] The results presented here seemingly indicate that the 'product state' of the reaction becomes entropically stabilized, $\Delta S^{\ddagger}$ = -90 J mol$^{-1}$ K$^{-1}$ while the initial state remains relatively unchanged, $\Delta S^{\ddagger}$ = -70 J mol$^{-1}$ K$^{-1}$, consistent with previous work.[**66**] Ultimately, this provides the standard entropy change garnered from the van't Hoff analysis.

As a final point, electron transfer reactions that are adiabatic contain a unique set of theoretical challenges. Under adiabatic assumptions, solvent-controlled electron transfer rates represent exceptions to the traditional Born-Oppenheimer approximation as the electronic structure dynamics, rate-limited by solvent, exists in a steady-state with the solvent dielectric as it traverses the potential energy surface.[69-71] The fact that such violations occur, and as a consequence solvent-controlled rates begin to arise, may explain the origin of the enthalpic barriers observed for the adiabatic reactions closely matching the barrier for solvent longitudinal motion, $\Delta H_L^{\ddagger}$.[34] An additional concern for an adiabatic electron transfer reaction is that motion through the transition state is repeated or initial crossing of the barrier fails as a result of solvent influence – an effect not typically observed for non-adiabatic electron transfer.[**72**] This would also manifest through a more negative activation entropy as a specific local solvent arrangement of orbitals facilitates the reaction, an entropically unfavorable event.

**Conclusion**: In summary, the kinetics for electron transfer reactions in a strong (adiabatic) and weak (non-adiabatic) electronic coupling regime were analyzed with Eyring and Marcus continuum theories. Placed into context, the results indicate that even though coupling accelerates the electron transfer rate constant by allowing a rapid approach to the transition state, a substantial entropic penalty is imposed despite smaller $\Delta H^{\ddagger}$ for thermodynamically uphill reactions. Entropies of activation were dissected into nuclear and electronic components and the degree of (non-)adiabaticity was accounted for through the transmission coefficient ($\kappa_{el}$, Eyring) or Jortner adiabaticity parameter, ($\kappa_a$, Marcus). Free energy barriers were found to be independent of the coupling, despite a theoretical expectation that $H_{DA}$ reduces the barrier. Finally, $\Delta S^{\ddagger}$ was found to be a significant contributor to the activation energy. The thermodynamic quantities were placed into context using previous studies on bimolecular, biological, and bridged inter- and intramolecular electron transfer. The work presented here is an early example of explicit characterization of both forward and reverse rates of thermal electron transfer reactions that lie in extreme regimes of electron transfer theory and which are relevant to energy conversion schemes.

## Associated Content

Supporting Information: The Supporting Information is available free of charge on the ACS Publications website.

Dielectric continuum theory calculation of the reorganization energy, adiabatic and non-adiabatic rate constant calculations, temperature dependence of the solvent reorientation time, Errors for standard thermodynamic properties, and derivation of the relationship between the Eyring and Marcus models.

## Author Information

Corresponding Author: [*]gjmeyer@email.unc.edu

Notes: [‡]These authors contributed equally. [†]Present address: Chemistry Division, Building 555, Brookhaven National Laboratory, Upton, NY 11973.

## Acknowledgements

The authors gratefully acknowledge support from the Division of Chemical Sciences, Office of Basic Energy Sciences, Office of Energy Research, US Department of Energy (Grant DE-SC0013461). L.T.-G. acknowledges the Belgian American Educational Foundation as well as the Bourse d'excellence Wallonie-Bruxelles International for postdoctoral funding.

## References:

1. Groot, M.-L.; van Mourik, F.; Eijckelhoff, C.; van Stokkum, I. H. M.; Dekker, J. P.; van Grondelle, R., Charge separation in the reaction center of photosystem II studied as a function of temperature. *Proc. Natl. Acad. Sci. USA* **1997,** *94* (9), 4389-4394.
2. Veldkamp, B. S.; Han, W.-S.; Dyar, S. M.; Eaton, S. W.; Ratner, M. A.; Wasielewski, M. R., Photoinitiated multi-step charge separation and ultrafast charge transfer induced dissociation in a pyridyl-linked photosensitizer–cobaloxime assembly. *Energy Environ Sci* **2013,** *6* (6), 1917-1928.
3. Lewis, F. D.; Wu, T.; Liu, X.; Letsinger, R. L.; Greenfield, S. R.; Miller, S. E.; Wasielewski, M. R., Dynamics of Photoinduced Charge Separation and Charge Recombination in Synthetic DNA Hairpins with Stilbenedicarboxamide Linkers. *J. Am. Chem. Soc.* **2000,** *122* (12), 2889-2902.
4. Troian-Gautier, L.; DiMarco, B. N.; Sampaio, R. N.; Marquard, S. L.; Meyer, G. J., Evidence that ΔS‡ Controls Interfacial Electron Transfer Dynamics from Anatase TiO2 to Molecular Acceptors. *J. Am. Chem. Soc.* **2018,** *140* (8), 3019-3029.
5. Marcus, R. A.; Sutin, N., Electron transfers in chemistry and biology. *Biochim. Biophys. Acta* **1985,** *811* (3), 265-322.
6. Isied, S. S.; Kuehn, C.; Worosila, G., Ruthenium-modified cytochrome c: temperature dependence of the rate of intramolecular electron transfer. *J. Am. Chem. Soc.* **1984,** *106* (6), 1722-1726.
7. Weiss, E. A.; Tauber, M. J.; Kelley, R. F.; Ahrens, M. J.; Ratner, M. A.; Wasielewski, M. R., Conformationally Gated Switching between Superexchange and Hopping within Oligo-p-phenylene-Based Molecular Wires. *J. Am. Chem. Soc.* **2005,** *127* (33), 11842-11850.
8. Roth, J. P.; Lovell, S.; Mayer, J. M., Intrinsic Barriers for Electron and Hydrogen Atom Transfer Reactions of Biomimetic Iron Complexes. *J. Am. Chem. Soc.* **2000,** *122* (23), 5486-5498.
9. Closs, G. L.; Miller, J. R., Intramolecular Long-Distance Electron Transfer in Organic Molecules. *Science* **1988,** *240* (4851), 440-447.
10. Nocera, D. G.; Winkler, J. R.; Yocom, K. M.; Bordignon, E.; Gray, H. B., Kinetics of intermolecular and intramolecular electron transfer from ruthenium(II) complexes to ferricytochrome c. *J. Am. Chem. Soc.* **1984,** *106* (18), 5145-5150.
11. Lear, B. J.; Glover, S. D.; Salsman, J. C.; Londergan, C. H.; Kubiak, C. P., Solvent Dynamical Control of Ultrafast Ground State Electron Transfer: Implications for Class II−III Mixed Valency. *J. Am. Chem. Soc.* **2007,** *129* (42), 12772-12779.

12. Londergan, C. H.; Salsman, J. C.; Ronco, S.; Dolkas, L. M.; Kubiak, C. P., Solvent Dynamical Control of Electron-Transfer Rates in Mixed-Valence Complexes Observed by Infrared Spectral Line Shape Coalescence. *J. Am. Chem. Soc.* **2002,** *124* (22), 6236-6237.
13. Sampaio, R. N.; Piechota, E. J.; Troian-Gautier, L.; Maurer, A. B.; Hu, K.; Schauer, P. A.; Blair, A. D.; Berlinguette, C. P.; Meyer, G. J., Kinetics teach that electronic coupling lowers the free-energy change that accompanies electron transfer. *Proc. Natl. Acad. Sci. USA* **2018,** *115* (28), 7248-7253.
14. Robson, K. C. D.; Sporinova, B.; Koivisto, B. D.; Schott, E.; Brown, D. G.; Berlinguette, C. P., Systematic Modulation of a Bichromic Cyclometalated Ruthenium(II) Scaffold Bearing a Redox-Active Triphenylamine Constituent. *Inorg. Chem.* **2011,** *50* (13), 6019-6028.
15. Piechota, E. J.; Troian-Gautier, L.; Sampaio, R. N.; Brennaman, M. K.; Hu, K.; Berlinguette, C. P.; Meyer, G. J., Optical Intramolecular Electron Transfer in Opposite Directions through the Same Bridge That Follows Different Pathways. *J. Am. Chem. Soc.* **2018,** *140* (23), 7176-7186.
16. Brunschwig, B. S.; Creutz, C.; Sutin, N., Optical transitions of symmetrical mixed-valence systems in the Class II–III transition regime. *Chem. Soc. Rev.* **2002,** *31* (3), 168-184.
17. Brunschwig, B. S.; Sutin, N., Energy surfaces, reorganization energies, and coupling elements in electron transfer. *Coord. Chem. Rev.* **1999,** *187* (1), 233-254.
18. Hu, K.; Blair, A. D.; Piechota, E. J.; Schauer, P. A.; Sampaio, R. N.; Parlane, F. G. L.; Meyer, G. J.; Berlinguette, C. P., Kinetic pathway for interfacial electron transfer from a semiconductor to a molecule. *Nat Chem* **2016,** *8* (9), 853-859.
19. Frauenfelder, H.; Wolynes, P., Rate theories and puzzles of hemeprotein kinetics. *Science* **1985,** *229* (4711), 337-345.
20. Hupp, J. T.; Weaver, M. J., Entropic driving-force effects upon preexponential factors for intramolecular electron transfer: implications for the assessment of nonadiabaticity. *Inorg. Chem.* **1984,** *23* (2), 256-258.
21. Creutz, C., Nonadiabatic, Short-Range, Intramolecular Electron Transfer from Ruthenium(II) to Cobalt(III) Complexes. *J. Phys. Chem. B* **2007,** *111* (24), 6713-6717.
22. Brunschwig, B. S.; Logan, J.; Newton, M. D.; Sutin, N., A semiclassical treatment of electron-exchange reactions. Application to the hexaaquoiron(II)-hexaaquoiron(III) system. *J. Am. Chem. Soc.* **1980,** *102* (18), 5798-5809.
23. Brown, G. M.; Sutin, N., A comparison of the rates of electron exchange reactions of ammine complexes of ruthenium(II) and -(III) with the predictions of adiabatic, outer-sphere electron transfer models. *J. Am. Chem. Soc.* **1979,** *101* (4), 883-892.
24. Bolton, J. R.; Archer, M. D., Basic Electron-Transfer Theory. In *Electron Transfer in Inorganic, Organic, and Biological Systems*, American Chemical Society: 1991; Vol. 228, pp 7-23.
25. Rips, I.; Jortner, J., Dynamic solvent effects on outer-sphere electron transfer. *J. Chem. Phys.* **1987,** *87* (4), 2090-2104.
26. Fawcett, W. R.; Fawcett, W. R., *Liquids, Solutions, and Interfaces : From Classical Macroscopic Descriptions to Modern Microscopic Details*. Oxford University Press: Cary, UNITED STATES, 2004.
27. Jortner, J.; Bixon, M., Intramolecular vibrational excitations accompanying solvent-controlled electron transfer reactions. *J. Chem. Phys.* **1988,** *88* (1), 167-170.
28. Sutin, N., Theory of Electron Transfer Reactions: Insights and Hindsights. In Progress in Inorganic Chemistry. In *Progress in Inorganic Chemistry,* Lippard, S. J., Ed. 2007.
29. Steinfeld, J. I. F., J. S.; Hase, W. L., *Chemical Kinetics and Dynamics*. 2nd ed.; Prentice Hall: New Jersey, 1998.
30. Kuss-Petermann, M.; Wenger, O. S., Electron Transfer Rate Maxima at Large Donor–Acceptor Distances. *J. Am. Chem. Soc.* **2016,** *138* (4), 1349-1358.
31. Farver, O.; Pecht, I., Low activation barriers characterize intramolecular electron transfer in ascorbate oxidase. *Proc. Natl. Acad. Sci. USA* **1992,** *89* (17), 8283-8287.
32. Larsen, C. B.; Wenger, O. S., Circular Photoinduced Electron Transfer in a Donor-Acceptor-Acceptor Triad. *Angew. Chem. Int. Ed.* **2018,** *57* (3), 841-845.
33. Zhong, Y.-W.; Gong, Z.-L.; Shao, J.-Y.; Yao, J., Electronic coupling in cyclometalated ruthenium complexes. *Coord. Chem. Rev.* **2016,** *312,* 22-40.

34. Manbeck, G. F.; Fujita, E.; Concepcion, J. J., Proton-Coupled Electron Transfer in a Strongly Coupled Photosystem II-Inspired Chromophore–Imidazole–Phenol Complex: Stepwise Oxidation and Concerted Reduction. *J. Am. Chem. Soc.* **2016,** *138* (36), 11536-11549.
35. Schäfer, J.; Holzapfel, M.; Mladenova, B.; Kattnig, D.; Krummenacher, I.; Braunschweig, H.; Grampp, G.; Lambert, C., Hole Transfer Processes in meta- and para-Conjugated Mixed Valence Compounds: Unforeseen Effects of Bridge Substituents and Solvent Dynamics. *J. Am. Chem. Soc.* **2017,** *139* (17), 6200-6209.
36. Londergan, C. H.; Salsman, J. C.; Lear, B. J.; Kubiak, C. P., Observation and dynamics of "mixed-valence isomers" and a thermodynamic estimate of electronic coupling parameters. *Chemical Physics* **2006,** *324* (1), 57-62.
37. Salsman, J. C.; Kubiak, C. P.; Ito, T., Mixed Valence Isomers. *J. Am. Chem. Soc.* **2005,** *127* (8), 2382-2383.
38. Maroncelli, M.; MacInnis, J.; Fleming, G. R., Polar Solvent Dynamics and Electron-Transfer Reactions. *Science* **1989,** *243* (4899), 1674-1681.
39. Weaver, M. J., Dynamical solvent effects on activated electron-transfer reactions: principles, pitfalls, and progress. *Chem. Rev.* **1992,** *92* (3), 463-480.
40. Liu, M.; Ito, N.; Maroncelli, M.; Waldeck, D. H.; Oliver, A. M.; Paddon-Row, M. N., Solvent Friction Effect on Intramolecular Electron Transfer. *J. Am. Chem. Soc.* **2005,** *127* (50), 17867-17876.
41. Newton, M. D.; Sutin, N., Electron Transfer Reactions in Condensed Phases. *Annual Review of Physical Chemistry* **1984,** *35* (1), 437-480.
42. Demadis, K. D.; Hartshorn, C. M.; Meyer, T. J., The Localized-to-Delocalized Transition in Mixed-Valence Chemistry. *Chem. Rev.* **2001,** *101* (9), 2655-2686.
43. Hush, N. S., Intervalence-Transfer Absorption. Part 2. Theoretical Considerations and Spectroscopic Data. In *Progress in Inorganic Chemistry*, 2007.
44. Cave, R. J.; Newton, M. D., Generalization of the Mulliken-Hush treatment for the calculation of electron transfer matrix elements. *Chem. Phys. Lett.* **1996,** *249* (1), 15-19.
45. Yonemoto, E. H.; Riley, R. L.; Kim, Y. I.; Atherton, S. J.; Schmehl, R. H.; Mallouk, T. E., Photoinduced electron transfer in covalently linked ruthenium tris(bipyridyl)-viologen molecules: observation of back electron transfer in the Marcus inverted region. *J. Am. Chem. Soc.* **1992,** *114* (21), 8081-8087.
46. Fox, L. S.; Kozik, M.; Winkler, J. R.; Gray, H. B., Gaussian Free-Energy Dependence of Electron-Transfer Rates in Iridium Complexes. *Science* **1990,** *247* (4946), 1069-1071.
47. Moia, D.; Vaissier, V.; López-Duarte, I.; Torres, T.; Nazeeruddin, M. K.; O'Regan, B. C.; Nelson, J.; Barnes, P. R. F., The reorganization energy of intermolecular hole hopping between dyes anchored to surfaces. *Chemical Science* **2014,** *5* (1), 281-290.
48. Biner, M.; Buergi, H. B.; Ludi, A.; Roehr, C., Crystal and molecular structures of [Ru(bpy)3](PF6)3 and [Ru(bpy)3](PF6)2 at 105 K. *J. Am. Chem. Soc.* **1992,** *114* (13), 5197-5203.
49. Cias, P.; Slugovc, C.; Gescheidt, G., Hole Transport in Triphenylamine Based OLED Devices: From Theoretical Modeling to Properties Prediction. *The Journal of Physical Chemistry A* **2011,** *115* (50), 14519-14525.
50. Åqvist, J.; Kazemi, M.; Isaksen, G. V.; Brandsdal, B. O., Entropy and Enzyme Catalysis. *Accounts of Chemical Research* **2017,** *50* (2), 199-207.
51. Armstrong, A. A.; Amzel, L. M., Role of Entropy in Increased Rates of Intramolecular Reactions. *J. Am. Chem. Soc.* **2003,** *125* (47), 14596-14602.
52. Page, M. I.; Jencks, W. P., Entropic Contributions to Rate Accelerations in Enzymic and Intramolecular Reactions and the Chelate Effect. *Proc. Natl. Acad. Sci. USA* **1971,** *68* (8), 1678-1683.
53. Bruice, T. C.; Lightstone, F. C., Ground State and Transition State Contributions to the Rates of Intramolecular and Enzymatic Reactions. *Accounts of Chemical Research* **1999,** *32* (2), 127-136.
54. Villà, J.; Štrajbl, M.; Glennon, T. M.; Sham, Y. Y.; Chu, Z. T.; Warshel, A., How important are entropic contributions to enzyme catalysis? *Proc. Natl. Acad. Sci. USA* **2000,** *97* (22), 11899-11904.
55. Motley, T. C.; Meyer, G. J., Intramolecular Electronic Coupling Enhances Lateral Electron Transfer across Semiconductor Interfaces. *The Journal of Physical Chemistry C* **2018,** *122* (26), 14420-14424.
56. DiMarco, B. N.; Motley, T. C.; Balok, R. S.; Li, G.; Siegler, M. A.; O'Donnell, R. M.; Hu, K.; Meyer, G. J., A Distance Dependence to Lateral Self-Exchange across Nanocrystalline TiO2. A Comparative Study of Three Homologous RuIII/II Polypyridyl Compounds. *The Journal of Physical Chemistry C* **2016,** *120* (26), 14226-14235.

57. Hu, K.; Meyer, G. J., Lateral Intermolecular Self-Exchange Reactions for Hole and Energy Transport on Mesoporous Metal Oxide Thin Films. *Langmuir* **2015,** *31* (41), 11164-11178.
58. Vaissier, V.; Barnes, P.; Kirkpatrick, J.; Nelson, J., Influence of polar medium on the reorganization energy of charge transfer between dyes in a dye sensitized film. *Phys. Chem. Chem. Phys.* **2013,** *15* (13), 4804-4814.
59. Brennan, B. J.; Regan, K. P.; Durrell, A. C.; Schmuttenmaer, C. A.; Brudvig, G. W., Solvent Dependence of Lateral Charge Transfer in a Porphyrin Monolayer. *ACS Energy Letters* **2017,** *2* (1), 168-173.
60. Cappel, U. B.; Feldt, S. M.; Schöneboom, J.; Hagfeldt, A.; Boschloo, G., The Influence of Local Electric Fields on Photoinduced Absorption in Dye-Sensitized Solar Cells. *J. Am. Chem. Soc.* **2010,** *132* (26), 9096-9101.
61. Ardo, S.; Sun, Y.; Staniszewski, A.; Castellano, F. N.; Meyer, G. J., Stark Effects after Excited-State Interfacial Electron Transfer at Sensitized TiO2 Nanocrystallites. *J. Am. Chem. Soc.* **2010,** *132* (19), 6696-6709.
62. O'Donnell, R. M.; Sampaio, R. N.; Barr, T. J.; Meyer, G. J., Electric Fields and Charge Screening in Dye Sensitized Mesoporous Nanocrystalline TiO2 Thin Films. *The Journal of Physical Chemistry C* **2014,** *118* (30), 16976-16986.
63. Gennett, T.; Milner, D. F.; Weaver, M. J., Role of solvent reorganization dynamics in electron-transfer processes. Theory-experiment comparisons for electrochemical and homogeneous electron exchange involving metallocene redox couples. *J. Phys. Chem.* **1985,** *89* (13), 2787-2794.
64. Mader, E. A.; Manner, V. W.; Markle, T. F.; Wu, A.; Franz, J. A.; Mayer, J. M., Trends in Ground-State Entropies for Transition Metal Based Hydrogen Atom Transfer Reactions. *J. Am. Chem. Soc.* **2009,** *131* (12), 4335-4345.
65. Hupp, J. T.; Weaver, M. J., Solvent, ligand, and ionic charge effects on reaction entropies for simple transition-metal redox couples. *Inorg. Chem.* **1984,** *23* (22), 3639-3644.
66. Neyhart, G. A.; Timpson, C. J.; Bates, W. D.; Meyer, T. J., Solvent-Induced Electron Transfer and Electronic Delocalization in Mixed-Valence Complexes. Spectral Properties. *J. Am. Chem. Soc.* **1996,** *118* (15), 3730-3737.
67. Marcus, R. A.; Siders, P., Theory of highly exothermic electron transfer reactions. *J. Phys. Chem.* **1982,** *86* (5), 622-630.
68. Neyhart, G. A.; Hupp, J. T.; Curtis, J. C.; Timpson, C. J.; Meyer, T. J., Solvent-Induced Electron Transfer and Delocalization in Mixed-Valence Complexes. Electrochemistry. *J. Am. Chem. Soc.* **1996,** *118* (15), 3724-3729.
69. Hynes, J. T., Outer-sphere electron-transfer reactions and frequency-dependent friction. *J. Phys. Chem.* **1986,** *90* (16), 3701-3706.
70. Hynes, J. T., Chemical Reaction Dynamics in Solution. *Annual Review of Physical Chemistry* **1985,** *36* (1), 573-597.
71. Chen, P.; Meyer, T. J., Medium Effects on Charge Transfer in Metal Complexes. *Chem. Rev.* **1998,** *98* (4), 1439-1478.
72. Hans, H., Dynamic Solvent Effects on Electron-Transfer Reactions. *Angew. Chemie. Int. Ed* **1993,** *32* (3), 359-377.

## For Table of Contents Use Only: